

# DEUTSCHES ELEKTRONEN-SYNCHROTRON **DESY**

DESY 75/34  
September 1975



$e^+e^- \rightarrow$  Hadrons:

Results from the DESY-Heidelberg-Collaboration

presented by

J. Heintze

*Physikalisches Institut, Universität Heidelberg*

at the 1975 International Symposium  
on Lepton and Photon Interactions at  
High Energies, August 1975, Stanford University

2 HAMBURG 52 · NOTKESTIEG 1

To be sure that your preprints are promptly included in the  
HIGH ENERGY PHYSICS INDEX,  
send them to the following address ( if possible by air mail ) :

DESY  
Bibliothek  
2 Hamburg 52  
Notkestieg 1  
Germany

$e^+e^- \rightarrow$  HADRONS:

RESULTS FROM THE DESY-HEIDELBERG-COLLABORATION

J. HEINTZE

Physikalisches Institut, University of Heidelberg,  
Heidelberg, Germany

Abstract

Inclusive photon spectra and photon spectra for events with 4 prongs and 1  $\gamma$ -ray which result from the decay of the (3.1) and (3.7) resonances are presented. The decay (3.7)  $\rightarrow$  (3.1) +  $\gamma\gamma$  is observed confirming earlier results of the DASP collaboration. In an investigation of  $3\gamma$  final states, the decay modes (3.1) $\rightarrow\eta\gamma$  and (3.1) $\rightarrow\eta'\gamma$  are detected. In addition, the data indicate the existence of a new heavy mass particle at 2.75 GeV which decays into two photons. This conclusion is based on an analysis of the  $3\gamma$  events from (3.1) decays combining results of the DASP and of the DESY - Heidelberg collaboration.

---

Paper presented at the 1975 International Symposium on Lepton and Photon Interactions at High Energies, August 21-27, 1975, Stanford University



as well as for the cathode strips. In this way,  $(\phi, \theta)$  ambiguities can be removed in multiprong events.

The hodoscopes H and H' are composed of 64 counters in total, each counter covering an azimuthal interval  $\Delta\phi = 22.5^\circ$  and a polar angle interval  $\theta = 30^\circ-90^\circ$  or  $90^\circ-150^\circ$ . A track is identified by a coincidence between corresponding H, H' counters in the internal and external hodoscopes. Different track multiplicities can be selected by the trigger electronics.

A vessel made of epoxy-fibre glass is positioned between the second and the third chamber. It can be filled with mercury. Photons originating from the interaction point see a converter thickness of 2 radiation lengths. The coordinates of the conversion points are measured in the third chamber with accuracies  $\Delta\phi \approx \Delta\theta \approx 40$  mrad.

In order to identify electrons and photons and to measure their energies the cylindrical detector is surrounded by an arrangement of NaI (N) and lead glass counter blocks (L). The lead glass blocks on top and bottom have a dimension of 16 x 18 x 140 cm. Phototubes are fixed on both sides of these blocks to compensate light attenuation and to determine the shower position from the time difference. Each of the walls on both sides of the cylindrical detector consists of 12 NaI and 20 lead glass blocks. The NaI counters are used to improve the resolution for photon energies below 500 MeV. All pulse heights are added linearly in order to get a measurement of the energy deposited in the NaI and lead glass blocks. The NaI - lead glass counters cover a solid angle of  $\approx 60$  % of  $4\pi$ .

Muons are identified by drift chambers ( $\mu$ ) behind a 60 cm thick iron absorber. Cosmic rays can be identified by time of flight measurement between the scintillation counters (C). Close to the beam pipe two scintillation counter hodoscopes (M) of 16 elements each extend the solid angle for charged particles from 86 % to 95 % of  $4\pi$ . The scintillation counters (R) veto background triggers from the beam halo.

In the trigger we require several combinations of a certain minimum track multiplicity with a minimum energy deposited in the

NaI - lead glass counters (see table I). The on-line computer, a PDP 9, selects in a fast decision only events that originate from a zone near the interaction point.

<u>Table I</u>	<u>Number of prongs</u>	<u>Minimum Energy recorded</u>
	0	1500 MeV
	1	900 MeV
	2	400 MeV
	$\geq 3$	300 MeV

### III. Inclusive photon spectra

In order to obtain the inclusive photon spectra from the decays of the 3.1 GeV and 3.7 GeV resonances, we use only data without the mercury converter. The photon shower has to be inside an octant of the NaI - lead glass walls which is free from charged tracks. At 3.1 GeV (3.7 GeV) out of 53,000 (47,000) hadronic events 25,000 (22,000) had at least one photon fulfilling this criterion.

In Fig. 2 we show the photon energy spectra of both the (3.1)- and (3.7)-decays. They seem to be similar and both can be fitted to the sum of two exponentials with a change in slope at a photon energy of about 600 MeV. At the present state of the evaluation no quantitative conclusion is drawn since no corrections for the acceptance of the apparatus have been applied so far.

A search was made for events with a single photon associated to 4 charged tracks. Out of 22,000 events with photons (3.7 GeV, Fig. 2) 6,700 events had 4 prongs (Fig. 3) and 114 events had 4 prongs and 1 photon (Fig. 4). Most of these events are presumably still due to decays involving  $\pi^0$ 's. We estimate an upper limit ( $E_\gamma > 30$  MeV)

$$\frac{\Gamma (3.7) \rightarrow 4 \text{ charged} + 1\gamma}{\Gamma (3.7) \rightarrow \text{all}} < 3\%$$

The branching ratio for transitions involving monoenergetic  $\gamma$ -rays with an energy of  $\approx 200$  MeV and 4 prongs is  $< 1\%$  according to the data of Fig. 4.



The dashed curve in fig. 5b is a Monte Carlo calculation of this background. In order to study the background experimentally we included in the analysis events with at least one additional  $\gamma$ -ray recorded in the NaI - lead glass counters. These events were treated in the same way as our candidate events for reaction (1). In fig. 5c the effective mass of the  $e^+e^-$  system of the those events is plotted. A peak is observed at a central value of 3.3 GeV, in agreement with the Monte Carlo calculation.

Comparing the two figures we conclude that the peak at 3.1 GeV in fig. 5b has to be attributed to reaction (1). In the mass interval 3.0 - 3.2 GeV we find 20 events with an estimated background of 5 events. According to the  $\gamma\gamma$  opening angle distribution only a small fraction of these events can be due to the decay  $(3.7) \rightarrow (3,1) + \eta, \eta \rightarrow 2\gamma$ .

We conclude that we observe the same type of events as the ones reported in Ref. 4. Such events can be considered as evidence for the existence of an intermediate state  $P_C$ . A preliminary estimate gives a branching ratio of a few percent for the  $2\gamma$  - cascade. A more detailed evaluation including the energy measurements of the two photons is in progress.

#### V. $e^+e^- \rightarrow 3\gamma$ at 3.1 GeV and 3.7 GeV

We have searched for  $3\gamma$  events in the data taken at 3.1 GeV and 3.7 GeV, in order to investigate decays of the type

$$(3.1), (3.7) \rightarrow \gamma + m, \quad m \rightarrow \gamma + \gamma,$$

$m$  being an  $\eta, \eta'$ , or a new heavy-mass state. These decay modes have to be discriminated against the QED process  $e^+e^- \rightarrow 3\gamma$  and against other decays with more than 3 photons in the final state.

From the data recorded with the Hg-converter, we selected  $3\gamma$ -event candidates requiring (1) three conversion points seen in the cylindrical detector, (2) a recorded energy  $> 50$  MeV behind



each conversion point, (3) no uncorrelated energy seen in the NaI and lead-glass counters, and (4) unique assignment of  $\phi$ ,  $\theta$  coordinates to each conversion point.

All candidates were analyzed assuming that they are  $3\gamma$  events. The reconstruction was performed using the coordinates of the three conversion points and assuming energy and momentum conservation. The analysis yielded the three photon energies and the coordinate  $Z$  of the interaction point along the beam axis. Figure 6 shows the  $Z$ -distribution of the  $3\gamma$  events as well as of background events (4 photons seen and 1 photon ignored). As a reference, we show in Fig. 6c the vertex distribution of events from the QED process  $e^+e^- \rightarrow 2\gamma$ . From the comparison of these distributions we conclude that the 3 photon events are contaminated only by a minor background due to multiple photon events. A cut was applied to eliminate events with  $|Z| > 25$  mm. The correct reconstruction of the events was tested by comparing the calculated photon energies with the measured ones. About 5% of the events were rejected because of inconsistent energies<sup>5)</sup>.

A total of 47 events  $e^+e^- \rightarrow 3\gamma$  were found. 13 events were recorded at 3.7 GeV (integrated luminosity  $\approx 400$  nb<sup>-1</sup>), 34 events at 3.1 GeV ( $\approx 240$  nb<sup>-1</sup>) and no event at 3.05 GeV ( $\approx 24$  nb<sup>-1</sup>).

Three different invariant masses  $m_{\gamma\gamma}$  are obtained for each event. In a fully symmetric Dalitz plot,  $m_{12}^2$  vs.  $m_{13}^2$ , every event gives 6 points. In order to obtain a Dalitz plot with only 1 point per event, we plotted the lowest  $m^2$  vs. the highest  $m^2$ , confining the points to the hatched triangle in Fig. 7. If the  $3\gamma$  decay proceeds via an intermediate state with mass  $m$ , the points should accumulate along the trajectories indicated in Fig. 7. The density of points should be constant along each of the straight lines in the original Dalitz plot  $m_{12}^2$  vs.  $m_{13}^2$ . If the three photons come from the QED process  $e^+e^- \rightarrow 3\gamma$ , a completely different distribution is expected. Monte Carlo calculations of this process have been performed for  $\sqrt{s} = 3.1$  GeV and  $\sqrt{s} = 3.7$  GeV<sup>6)</sup>. Results are shown in Fig. 8.

The detection efficiency for  $3\gamma$  events is approximately constant in the whole Dalitz plot except the corner with the highest

values of  $m_H^2$ . Above  $m_H^2 = 9 \text{ GeV}^2$  at 3.1 GeV and above  $m_H^2 = 13 \text{ GeV}^2$  at 3.7 GeV, the soft photon has an energy below 100 MeV. The efficiency is reduced in this corner.

The Dalitz plot of  $3\gamma$  events observed at 3.7 GeV is shown in Fig. 9. The distribution is compatible with the Monte Carlo calculation for the QED process. Also, the absolute number of events agrees within a factor of two with the QED prediction. A more accurate comparison is not possible at present, since we have not yet determined the efficiency of the event selection criteria. One event is possibly due to the decay  $(3.7) \rightarrow \gamma\eta$ .

The Dalitz plot for the  $3\gamma$  events observed at 3.1 GeV exhibits a more interesting structure. Similar observations have been made by the DASP collaboration.<sup>2</sup> Figure 10 shows the Dalitz plot of the events observed in both experiments. The bands for the reaction  $(3.1) \rightarrow \gamma\eta$  and  $(3.1) \rightarrow \gamma\eta'$  are indicated. The widths correspond to estimates of the experimental error. Both in the DASP and in the DESY-Heidelberg experiment, accumulations of events in the  $\eta$  band and at high values of  $m_H^2$  are observed. Some events lie in the  $\eta'$  band. In the following, an analysis of the Dalitz plot, combining the results of both experiments, is presented.

Since at high masses there is a region of possible confusion, we analyze first the part of the Dalitz plot with  $m_H^2 < 6.8 \text{ GeV}^2$ . There are 12 events within the  $\eta$  band, 3 events within the  $\eta'$  band and 9 events outside these bands. These latter events are probably due to the QED reaction<sup>7)</sup>. The population of this part of the Dalitz plot can therefore be explained in terms of  $(3.1) \rightarrow \eta\gamma$ ,  $(3.1) \rightarrow \eta'\gamma$  and  $e^+e^- \rightarrow 3\gamma$  (QED).

Taking into account that 46% of the  $\eta$  band and 57% of the  $\eta'$  band are below  $m_H^2 = 6.8 \text{ GeV}^2$  and correcting for the different branching fractions of  $\eta \rightarrow 2\gamma$  and  $\eta' \rightarrow 2\gamma$  a ratio

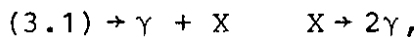
$$\frac{(3.1) \rightarrow \gamma\eta'}{(3.1) \rightarrow \gamma\eta} = 4 \pm 2.5$$

is obtained.

In the further analysis of the events, we consider the  $m_H^2$  distribution for all events within the  $\eta$  band (Fig. 11a) and for the events outside the  $\eta$  band (Fig. 11b). The distribution of the events is approximately flat. Within the  $\eta$  band, most events with  $m_H^2 > 6.8 \text{ GeV}^2$  can, therefore, be attributed to the decay  $(3.1) \rightarrow \gamma\eta$ . The distribution of the events outside the  $\eta$  band has a bump at  $7.5 \text{ GeV}^2$ , which is compatible neither with the flat distribution expected for events from the decay  $(3.1) \rightarrow \gamma\eta'$  nor with the smoothly rising distribution expected for QED events (Fig. 11c).

The interval  $6.8 \text{ GeV}^2 < m_H^2 < 8.2 \text{ GeV}^2$  contains 24 events.  $2 \pm 1.5$  events  $(3.1) \rightarrow \eta'\gamma$  are expected, assuming a flat distribution within the  $\eta'$  band. The QED background can be determined without absolute efficiency calculations using either the  $3\gamma$  events recorded outside the resonance region or the  $3\gamma$  events recorded at  $3.7 \text{ GeV}$ , assuming that all of these events are due to QED<sup>7)</sup>. Both methods show that the QED process contributes  $\leq 6$  events to the interval  $6.8 \text{ GeV}^2 < m_H^2 < 8.2 \text{ GeV}^2$ . There remains an excess of  $\sim 16$  events above the background of 6 to 10 events. The statistical probability for finding 24 events or more, when 10 events are expected, is  $\approx 3 \times 10^{-3}$ .

It can be seen in Fig. 10 that the excess of events at high values of  $m_H^2$  is uniformly spread in the Dalitz plot along a vertical line near  $m_H^2 = 7.5 \text{ GeV}^2$ . This suggests the existence of a state X with  $m_X = 2.75 \text{ GeV}$ . A Monte Carlo calculation for the decay mode,



resulted in a  $m_H^2$  distribution which is compatible with the data (dashed line in Fig. 11b). If the excess of events is attributed to such a state X, we obtain a ratio,

$$\frac{(3.1) \rightarrow \gamma + X}{(3.1) \rightarrow \gamma + \eta} \cdot \frac{\text{Branching ratio } (X \rightarrow 2\gamma)}{\text{Branching ratio } (\eta \rightarrow 2\gamma)} \approx 1$$

Summarizing the above discussion of the DASP and DESY-Heidelberg data, we conclude that at 3.1 GeV the number of observed  $3\gamma$  events and their distribution in the Dalitz plot cannot fully be explained by the three processes  $e^+e^- \rightarrow 3\gamma$  (QED),  $(3.1) \rightarrow n\gamma$  and  $(3.1) \rightarrow n'\gamma$ . There remains an excess of 16 events which indicates the existence of a heavy mass state X with  $m_X \approx 2.75$  GeV, which is produced by a radiative decay of the  $(3.1)$  resonance and which decays into two  $\gamma$  rays.

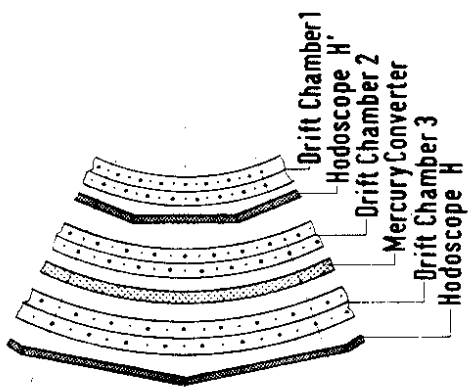
Note added in proof: The latest evaluation of the DASP Collaboration added three more events to the sample of  $3\gamma$ -decays. One event is a  $(3.1) \rightarrow \gamma n$  decay, one event is a candidate for  $(3.1) \rightarrow \gamma X(2750)$ ; the third event has solutions for  $(3.1) \rightarrow \gamma n$  as well as for  $(3.1) \rightarrow \gamma X(2750)$ .

## Footnotes and References

- 1) W. Bartel, P. Duinker, P. Steffen (DESY, Hamburg), and J. Heintze, G. Heinzelmann, R.D. Heuer, R. Mundhenke, H. Rieseberg, A. Wagner, A.H. Walenta (Physikal. Institut der Universität Heidelberg, Germany), and B. Schürlein (now at IDAS GmbH, Limburg/Lahn).
- 2) B. Wiik:  $e^+e^- \rightarrow$  Hadrons: DORIS results. Paper presented at the 1975 Lepton Photon Symposium, Stanford.
- 3) J. Heintze and A.H. Walenta, Nucl.Instr. and Meth. 111 (1973) 461; A.H. Walenta, IEEC Transactions on Nuclear Science 22 (1975) 251; A.H. Walenta, RHEL/M/H21 (1972) 116
- 4) DASP-collaboration, W. Braunschweig, H.-U. Martyn, H.G. Sander, D. Schmitz, W. Sturm, and W. Wallraff (RWTH Aachen), and K. Berkelman, D. Cords, R. Felst, E. Gadermann, G. Grindhammer, H. Hultschig, P. Joos, W. Koch, U. Kötz, H. Krehbiel, D. Kreinick, J. Ludwig, K.-H. Mess, K.C. Moffeit, A. Petersen, G. Poelz, J. Ringel, K. Sauerberg, P. Schmüser, G. Vogel, B.H. Wiik, and G. Wolf (DESY, Hamburg), and G. Buschhorn, R. Kotthaus, U.E. Kruse, H. Lierl, H. Oberlack, K. Pretzl, and M. Schliwa (MPI für Physik u. Astrophysik, München), and S. Orito, T. Suda, Y. Totsuka, and S. Yamada (University of Tokyo), Phys. Letters 57 B (1975) 407
- 5) The measured photon energies were not used in a constrained fit since it is difficult to account for the energy loss due to the edge effects.
- 6) The Monte Carlo calculations were kindly performed by Dr.P.Bock, Heidelberg. The formulae given by Geshkenbein and Terent'ev, Sov. Journ. Nucl. Phys. 8 (1969) 321 were used.
- 7) The QED background can be determined by measurement of  $3\gamma$  events outside the resonances. In the combined data of both experiments 2 events with  $m_H^2 < 6.8 \text{ GeV}^2$  and 1 event with  $6.8 \text{ GeV}^2 \leq m_H^2 < 8.2 \text{ GeV}^2$  were found. The integrated luminosities were  $\sim 150 \text{ nb}^{-1}$  outside resonance and  $\sim 450 \text{ nb}^{-1}$  at the 3.1 GeV resonance. Consequently, 6 and 3 QED events are expected in the two  $m_H^2$  intervals. Alternatively, the QED background can be determined by assuming that all  $3\gamma$  events at 3.7 GeV are due to the QED process. Making use of the Monte Carlo calculations for relating the 3.7 GeV and the 3.1 GeV QED events to each other,  $\sim 5$  events are expected in each of the two  $m_H^2$  intervals.

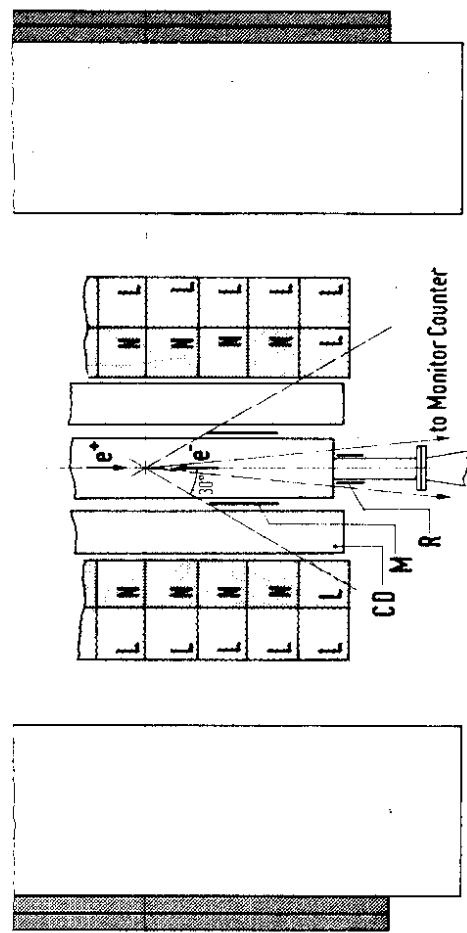
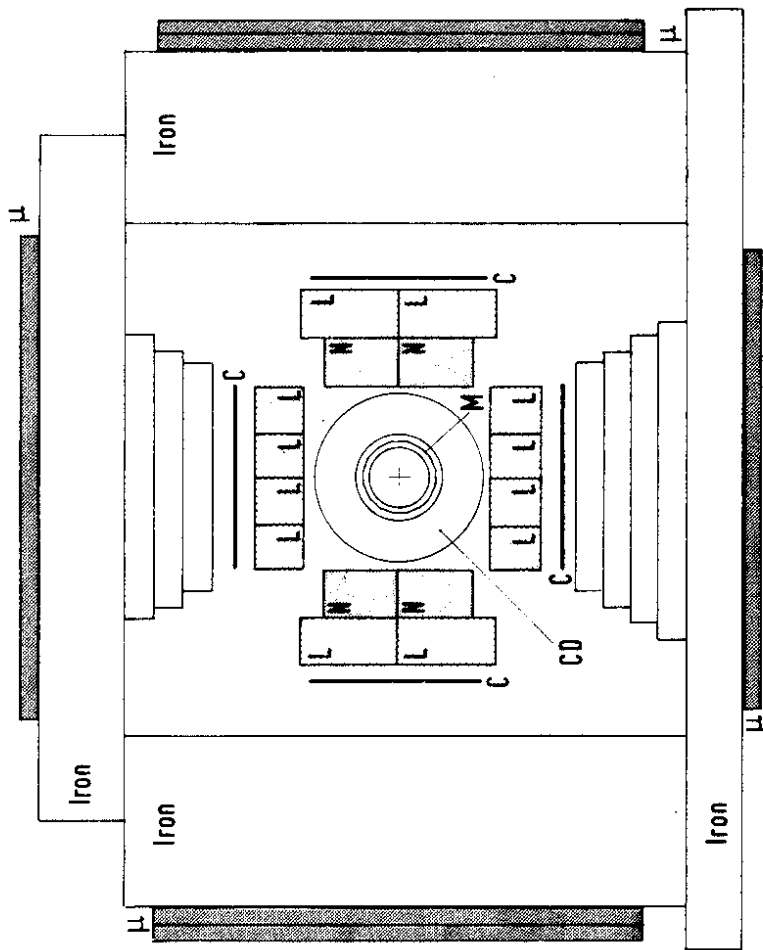
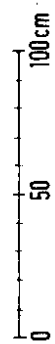
## Figure captions

1. Experimental apparatus
2. Inclusive photon spectra at 3.1 GeV and 3.7 GeV
3. Photon spectrum of 4 prong events
4. Photon spectra of events with 4 prongs and 1  $\gamma$ -ray. The dashed line indicates the resolution at 200 MeV.
5. (a) Photon cascade decay (3.7)  $\rightarrow$  (3.1)  
(b) Invariant mass distribution of  $e^+e^-$  pairs ( $e^+e^- \rightarrow e^+e^-\gamma\gamma$ )  
(c) Invariant mass distribution of  $e^+e^-$  pairs (background)
6. Distribution of reconstructed interaction points in beam direction.
7. Schematic Dalitz plot for  $3\gamma$  events.
8. Distribution of QED  $3\gamma$  events at 3.1 GeV. (Monte Carlo calculation, normalized to 100 events.)
9. Dalitz plot of  $3\gamma$  events recorded at 3.7 GeV. The numbers indicate the Monte Carlo prediction for the QED process normalized to the number of events observed below  $13 \text{ GeV}^2$ .
10. Dalitz plot of  $3\gamma$  events recorded at 3.1 GeV.
11. Distribution of  $3\gamma$  events along the  $m_H^2$ -axis in Fig. 8 and Fig. 10.
  - (a) Events within the  $\eta$  band
  - (b) Events outside the  $\eta$  band
  - (c) QED events (Background in D.HD-experiment times 5).

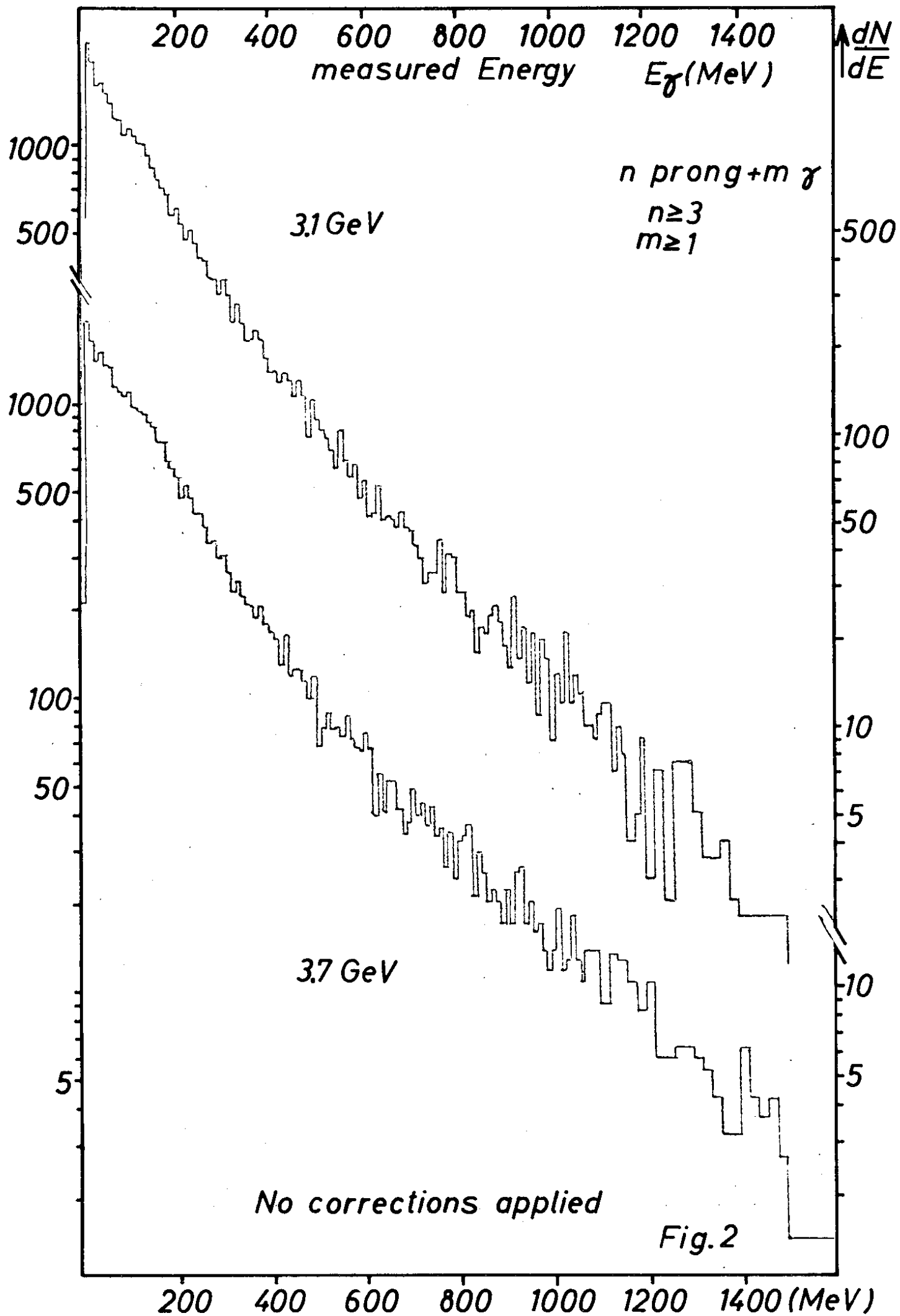


**Details of the  
Cylindrical Detector**

- W = NaI Counter
- L = Leadglass Counter
- $\mu$  = Muon Chamber
- CD = Cylindrical Detector
- C, M, R = Scintillation Counters



**Fig. 1**





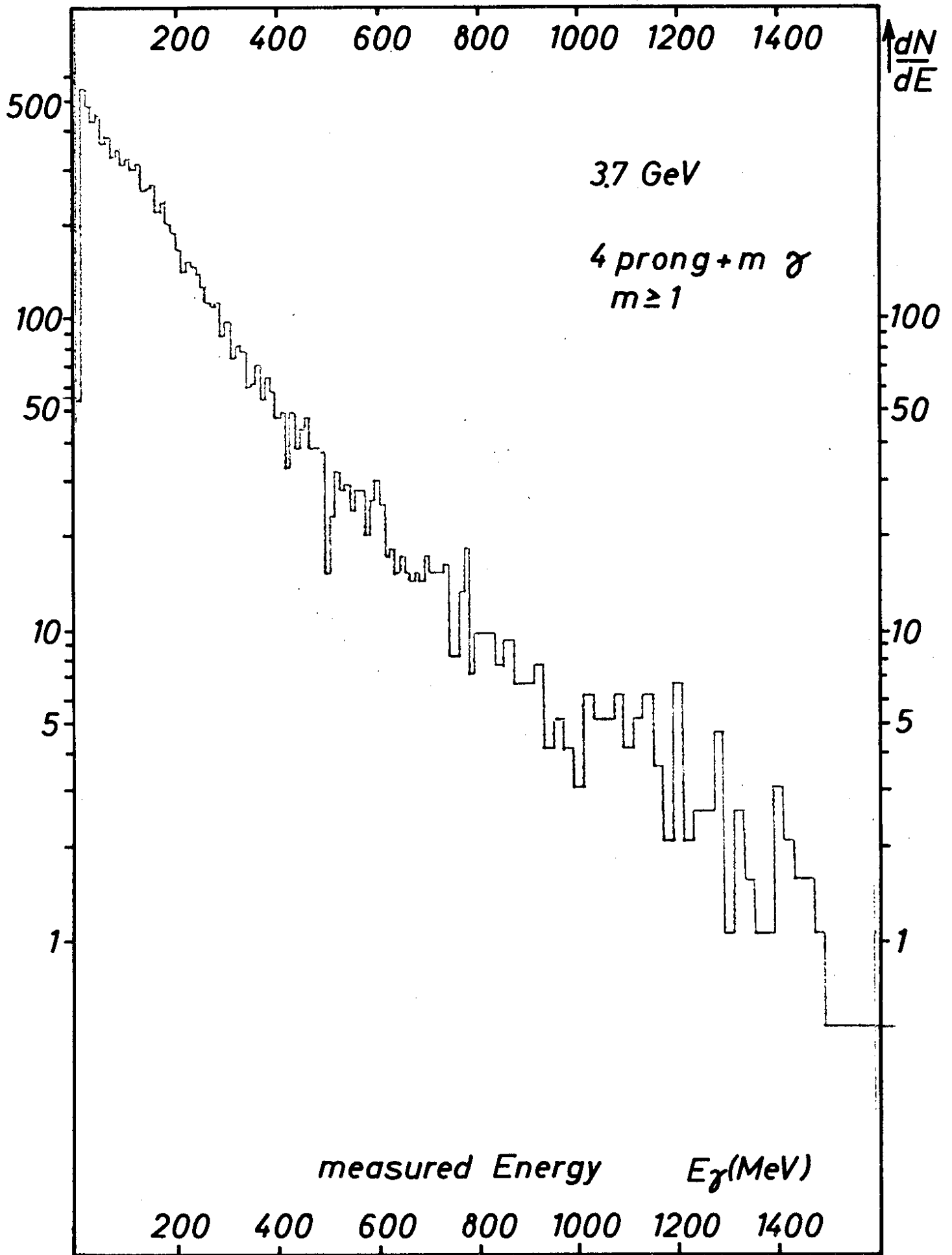


Fig.3

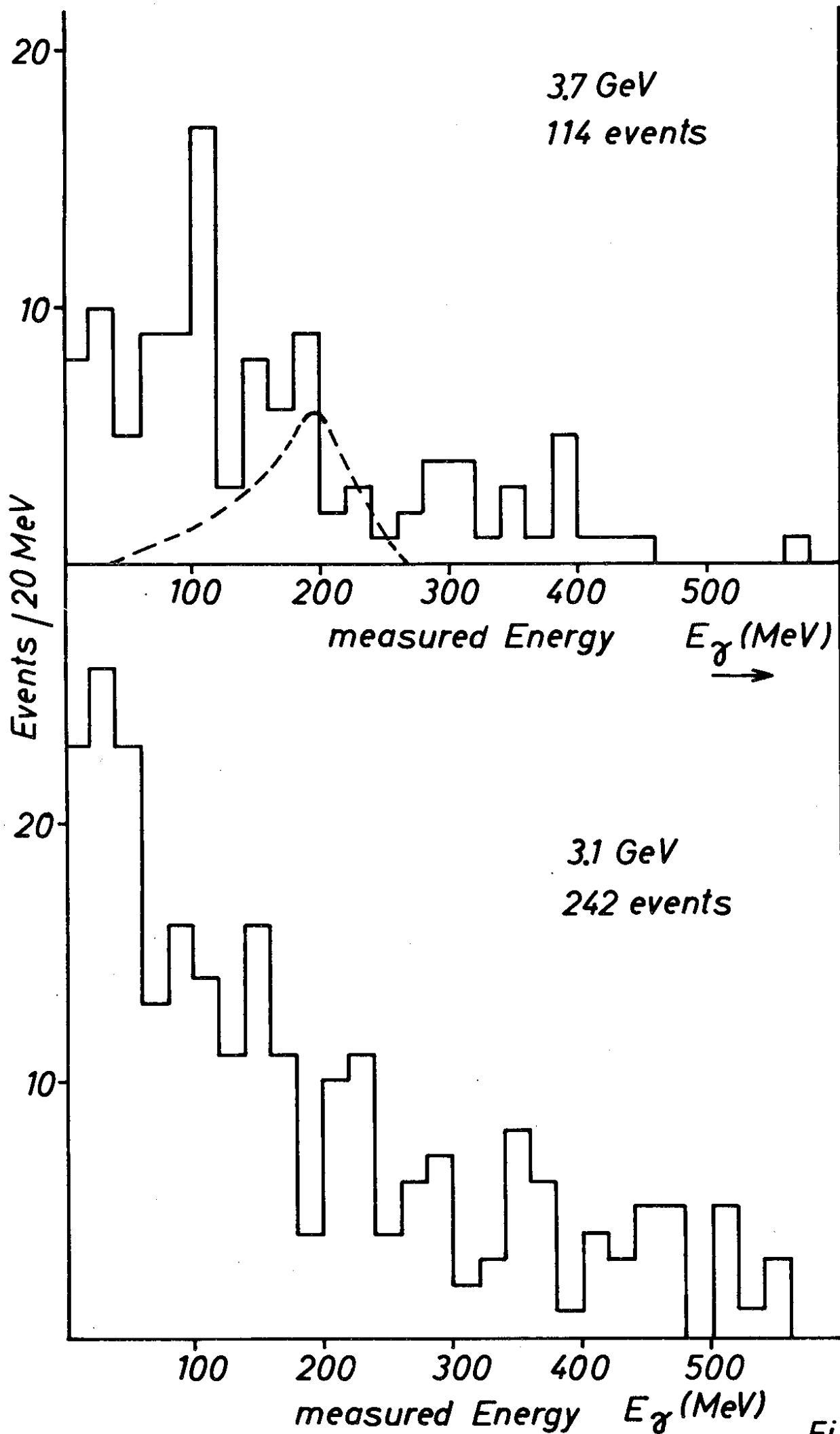


Fig. 4

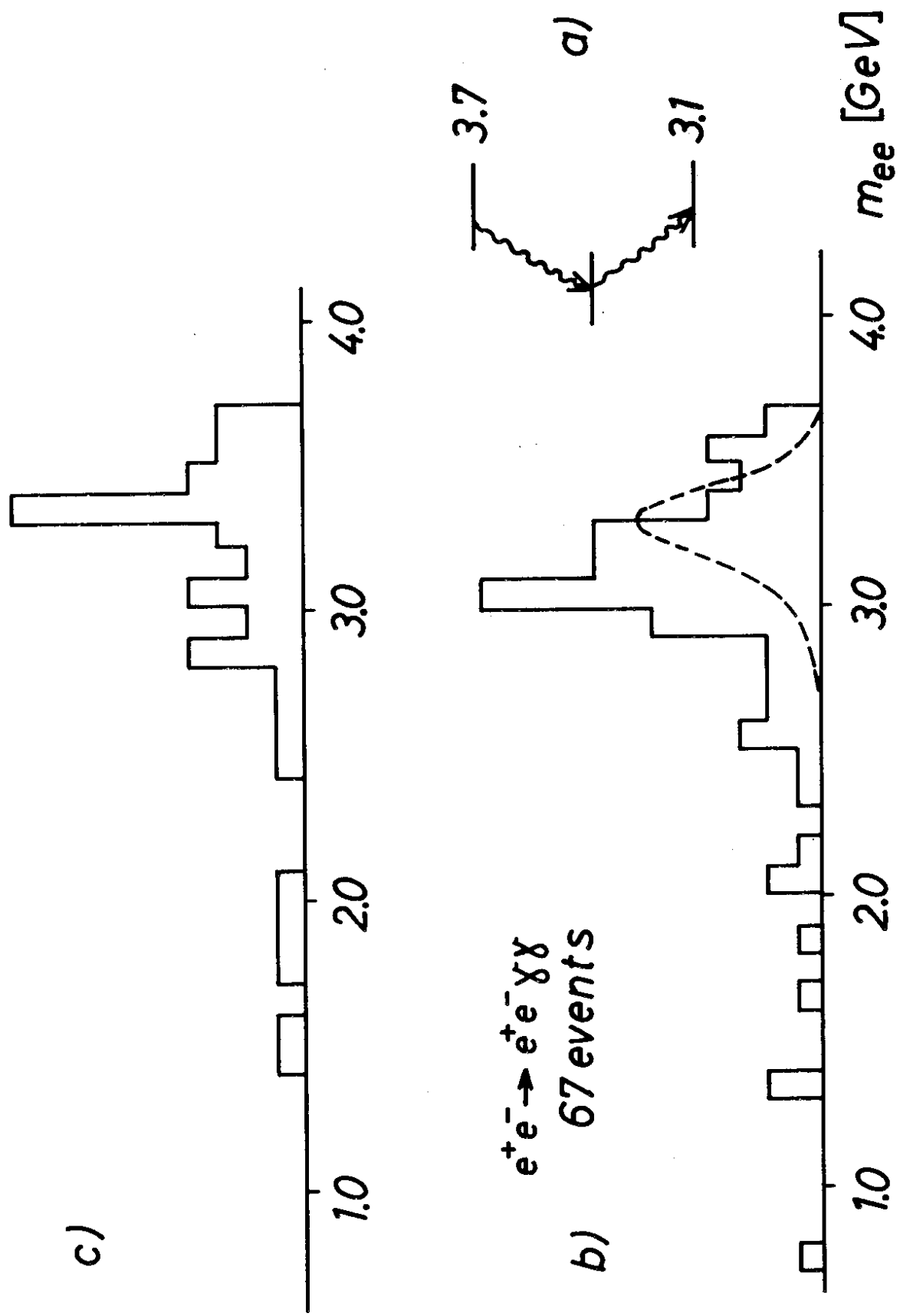
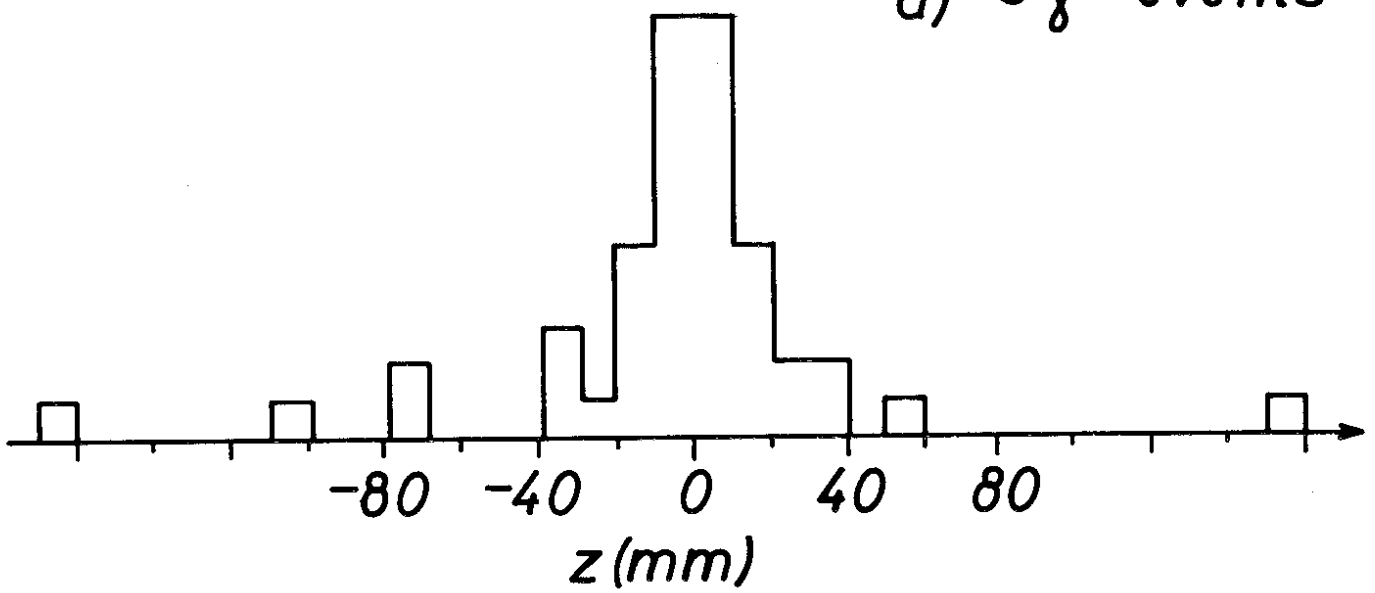
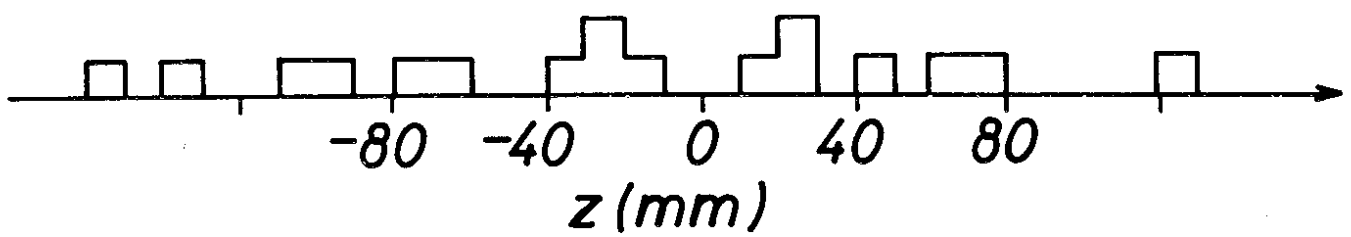


Fig. 5

a)  $3\gamma$ -events



b)  $4\gamma$  seen  
( $1\gamma$  ignored)



c)  $e^+e^- \rightarrow \gamma\gamma$

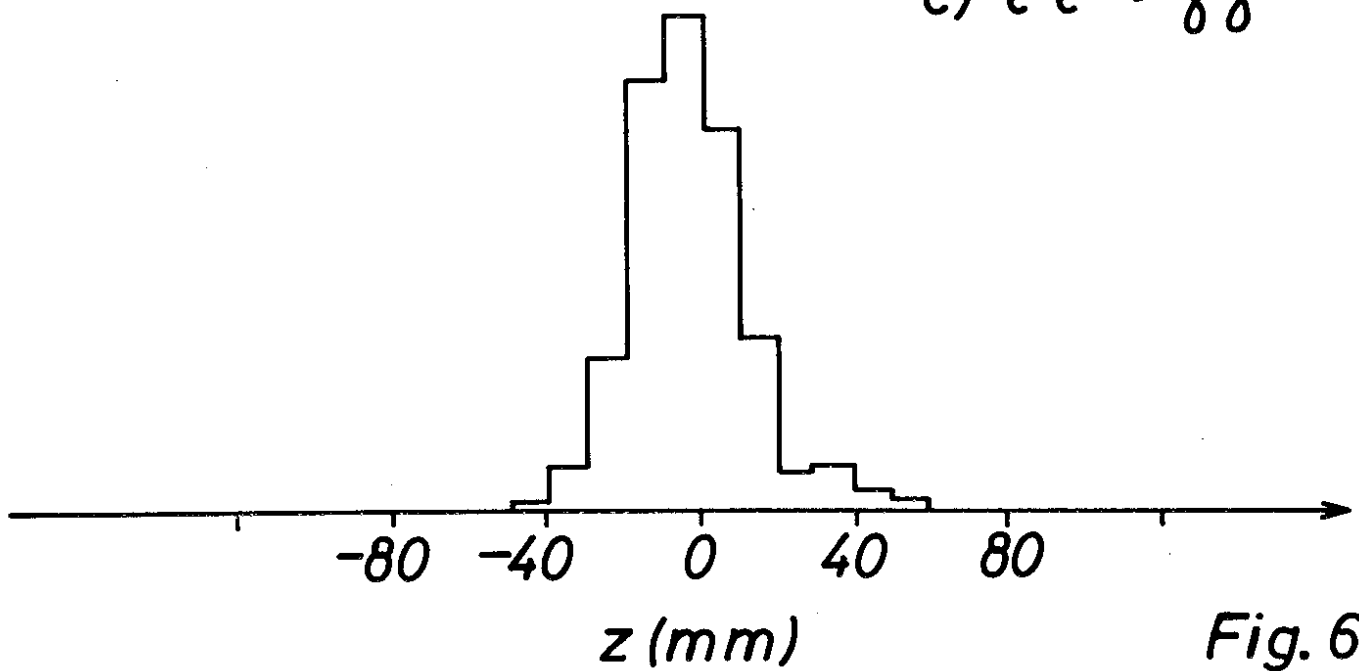


Fig. 6

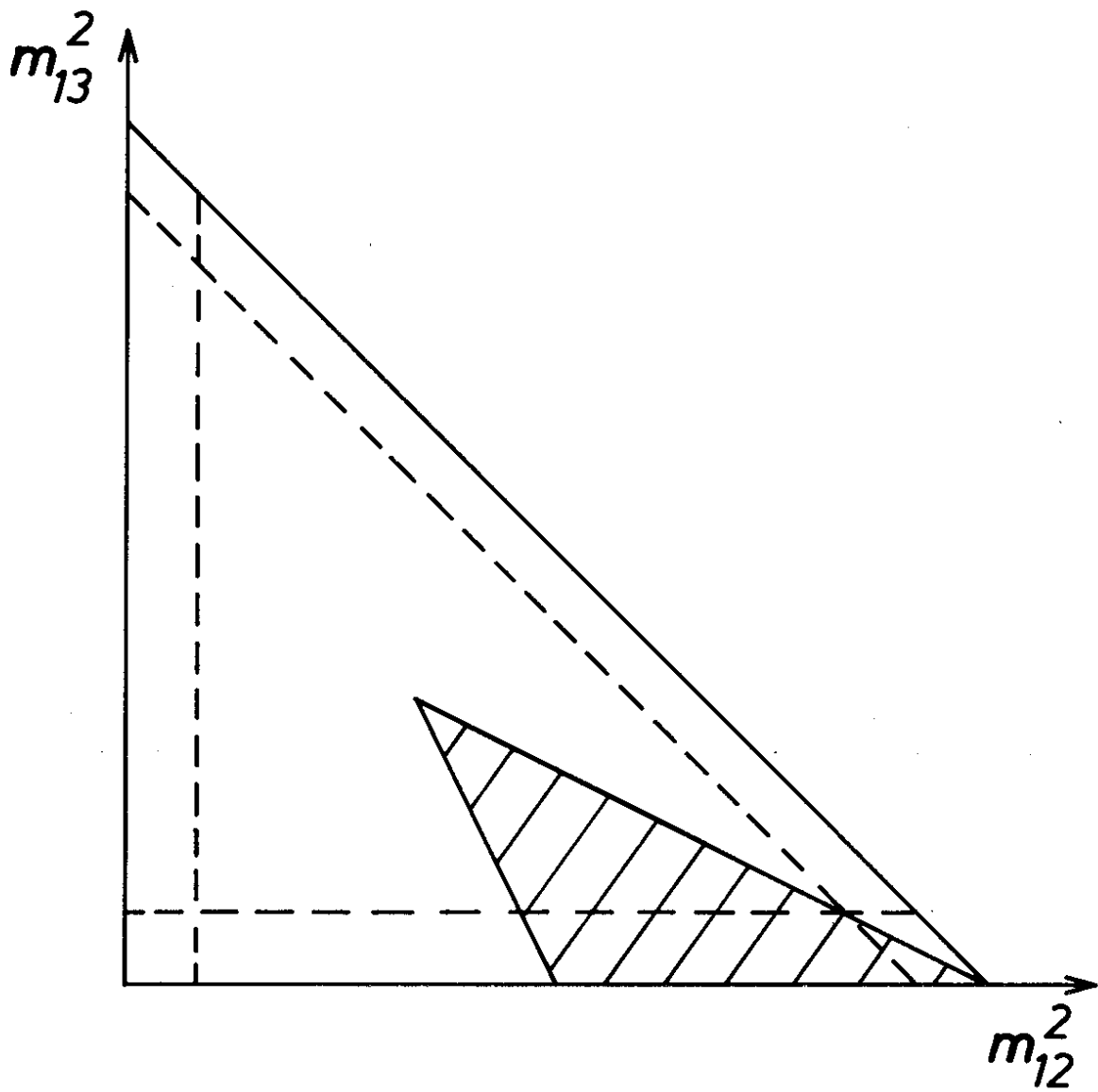


Fig. 7

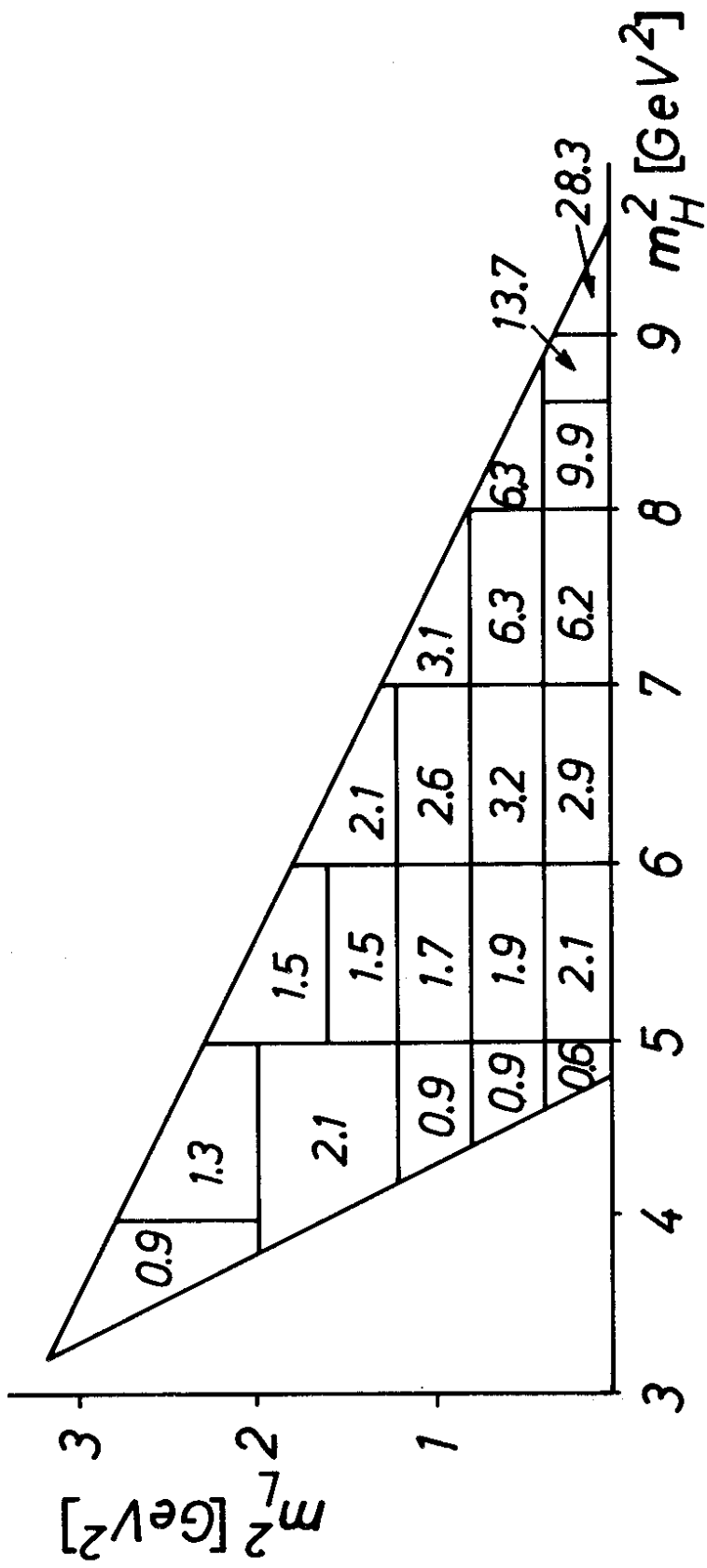


Fig. 8

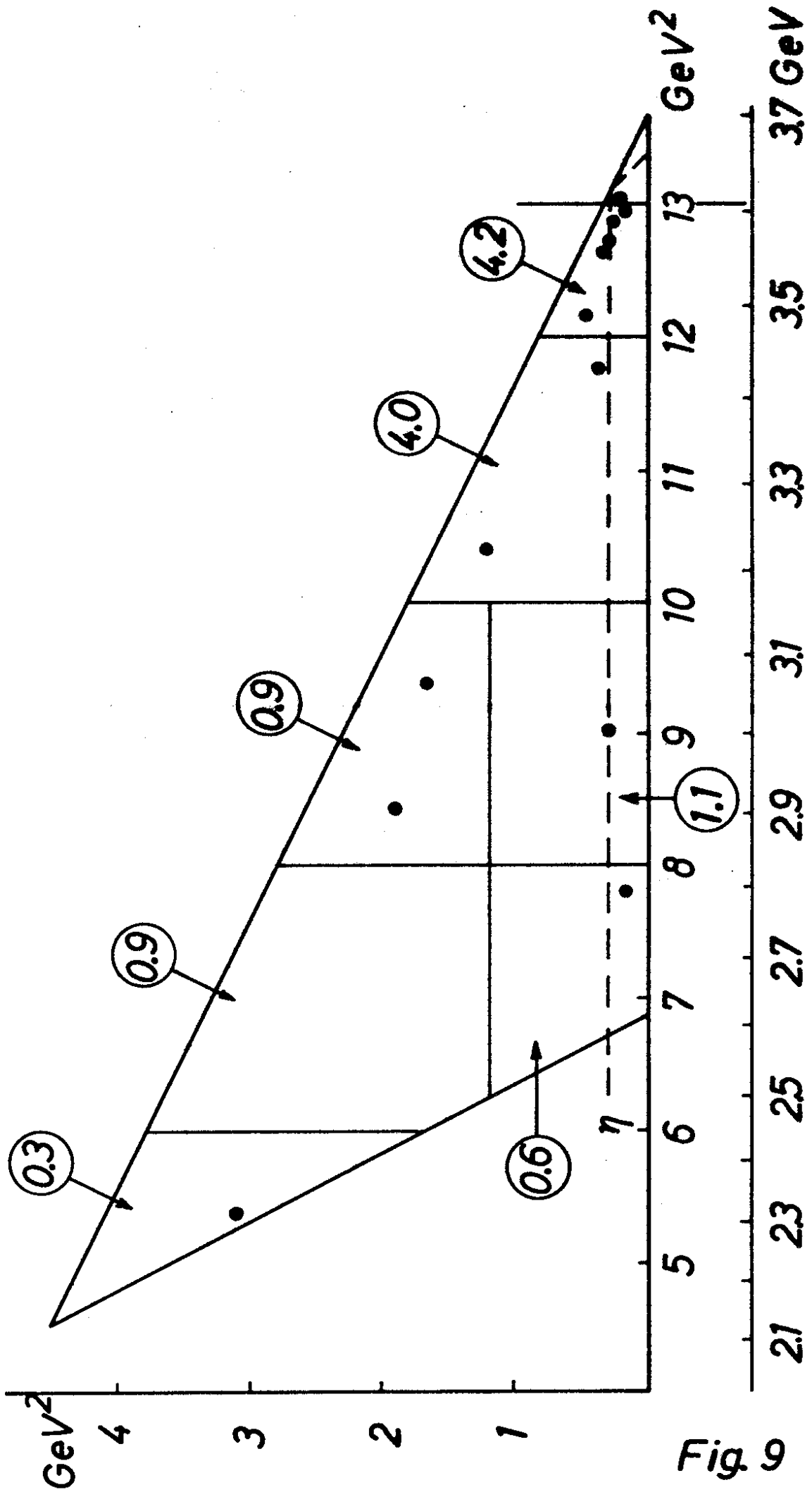


Fig. 9

× DASP  
 • DESY-HEIDELBERG

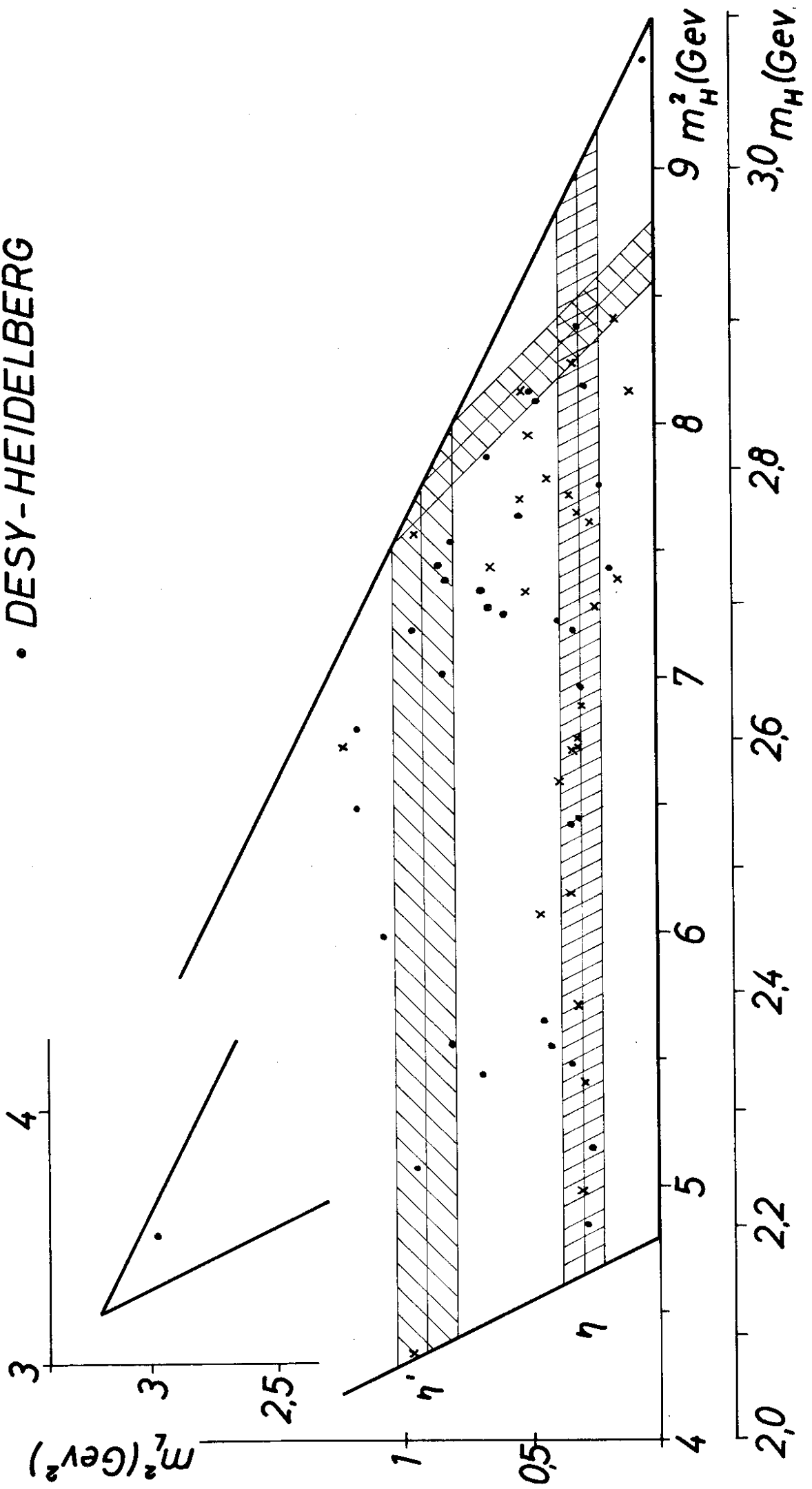


Fig 10



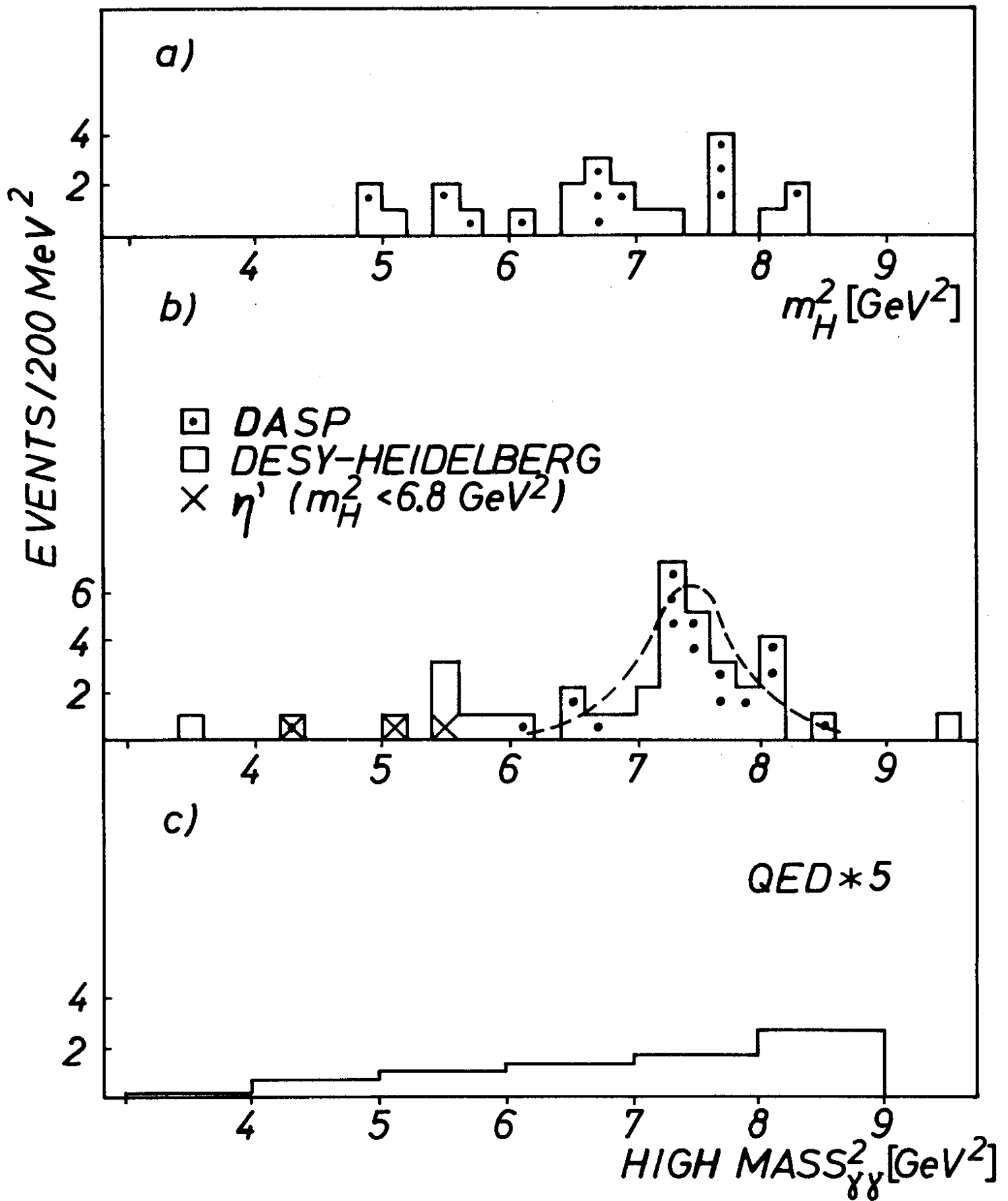


Fig. 11